Quantum Path Interference in the Wavelength Dependence of High-Harmonic Generation

K. Schiessl,[1,*] K. L. Ishikawa,[2,3] E. Persson,[1] and J. Burgdörfer[1]

[1]*Institute for Theoretical Physics, Vienna University of Technology, Wiedner Hauptstraße 8-10, A-1040 Vienna, Austria*

[2]*Department of Quantum Engineering and Systems Science, Graduate School of Engineering, University of Tokyo, Hongo 7-3-1, Bunkyo-ku, Tokyo 113-8656, Japan*

[3]*PRESTO (Precursory Research for Embryonic Science and Technology), Japan Science and Technology Agency, Honcho 4-1-8, Kawaguchi-shi, Saitama 332-0012, Japan*

(Received 21 August 2007; published 21 December 2007)

We investigate the dependence of the intensity of radiation due to high-harmonic generation as a function of the wavelength λ of the fundamental driver field. Superimposed on a smooth power-law dependence observed previously, we find surprisingly strong and rapid fluctuations on a fine λ scale. We identify the origin of these fluctuations in terms of quantum path interferences with up to five returning orbits significantly contributing.

DOI: 10.1103/PhysRevLett.99.253903 PACS numbers: 42.65.Ky, 32.80.Fb, 32.80.Rm

High-harmonic generation (HHG) represents a versatile and highly successful avenue towards an ultrashort coherent light source covering a wavelength range from the vacuum ultraviolet to the soft x-ray region [1]. HHG has successfully opened new research areas, such as attosecond science [2,3] and nonlinear optics in the extreme ultraviolet region [4,5]. The fundamental wavelength λ used in most of the existing HHG experiments is in the near-visible range ($\sim$800 nm). The cutoff law $E_c = |E_i| + 3.17U_p$, where $|E_i|$ denotes the binding energy of the target atom and $U_p = F_0^2/4\omega^2$ the ponderomotive energy (F_0, laser electric field strength), suggests that a longer fundamental wavelength is advantageous to extend the cutoff to a higher photon energy, since U_p quadratically increases with λ. There is an increasing interest in the development of high-power midinfrared ($\sim 2\ \mu$m) laser systems, e.g., based on optical parametric chirped pulse amplification. Along those lines the dependence of the HHG yield on λ has become an issue of major interest. It has been commonly accepted that the spreading of the returning wave packet would result in a λ^{-3} dependence of the HHG efficiency [6] as long as ground state depletion can be neglected [7]. Experimental findings [8] have provided partial support. Recently, however, Tate *et al.* [9] have reported a different wavelength scaling of HHG between 800 nm and 2 μm calculated with the time-dependent Schrödinger equation (TDSE) for Ar and a strong-field approximation (SFA) for He. They found a more rapidly decreasing HHG yield $\propto \lambda^{-x}$ with $5 \leq x \leq 6$. This surprising finding based on a somewhat limited number of data points motivated us to explore the λ dependence in more detail employing two completely independent integration methods of the TDSE to check for consistency and convergence. We have investigated the HHG for H and Ar on the level of single-atom response. Surprisingly, the harmonic yield does not smoothly decrease with fundamental wavelength but exhibits rapid oscillations with a period of 6–20 nm depending on the wavelength region. A semiclassical analysis based on the SFA reveals that the rapid oscillations are due to the interference of up to five different rescattering trajectories. Remarkably, averaged over the fast oscillations the smoothed yield follows an approximate λ^{-5} scaling, qualitatively consistent with the results of Tate *et al.* [9].

We solve the atomic time-dependent Schrödinger equation in a linearly polarized laser field in the length gauge,

$$i\frac{\partial}{\partial t}\psi(\mathbf{r}, t) = \left[-\frac{1}{2}\nabla^2 + V_{\text{eff}}(r) + zF(t)\right]\psi(\mathbf{r}, t), \quad (1)$$

where $F(t) = F_0 f(t)\sin(\omega t)$ denotes the laser electric field, $f(t)$ is the envelope function, and $V_{\text{eff}}(r)$ the atomic potential. For H, $V_{\text{eff}}(r)$ is the bare Coulomb potential while for Ar we employ a model potential [10] within the single-active electron approximation which reproduces the binding energy to an accuracy of typically $\approx 10^{-3}$. We employ two complementary methods to solve Eq. (1) in order to establish reliable and consistent results.

In the first method, Eq. (1) is numerically integrated using the alternating direction implicit (Peaceman-Rachford) method [11] with a uniform grid spacing Δr of 6.25×10^{-2} a.u. In order to reduce the difference between the discretized and analytical wave function, we scale the Coulomb potential by a few percent at the first grid point [12]. The time step Δt is 1/16000 of an optical cycle for 800 nm wavelength, i.e., 6.895×10^{-3} a.u. This algorithm is accurate to the order of $\mathcal{O}(\Delta t^3)$. In the second method, the TDSE is integrated on a finite grid by means of the pseudospectral method [13] which is also accurate to the order of $\mathcal{O}(\Delta t^3)$. It allows for time steps of the order of 0.1 a.u. The r coordinate is discretized within the interval $[0, r_{\max}]$ with a nonuniform mesh point distribution. The innermost grid point is typically as small as 2.5×10^{-4} a.u., enabling an accurate description near the nucleus. A smooth cutoff function is multiplied at each time step to avoid spurious reflections at the border $r_{\max}$, while equivalently another cutoff function prevents reflections at

the largest resolved energy E_{max}. Deeply bound, occupied states supported by the model potential are dynamically blocked during the time evolution by assigning a phase corresponding to an unphysically large and positive energy eigenvalue [14]. We calculate the dipole acceleration $\ddot{d}(t) = -\partial_t^2\langle z(t)\rangle$, employing the Ehrenfest theorem through the relation $\ddot{d}(t) = \langle\psi(\mathbf{r}, t) \mid \cos\theta/r^2 - F(t) \mid \psi(\mathbf{r}, t)\rangle$ [13], in which the second term can be dropped as it does not contribute to the HHG spectrum.

For a direct comparison we adopt the laser parameters of Ref. [9], with a fixed peak intensity of 1.6×10^{14} W/cm^2, a variation of λ between 800 nm and 2 μm, and an envelope function $f(t)$ corresponding to an 8-cycle flattop sine pulse with a half-cycle turn on and turn off. We have checked that the fluctuations in the harmonic yield to be discussed below are not an artifact of this particular choice of $f(t)$. They can be observed also for "smoother" pulse shape such as a $\sin^2$ pulse, provided that the pulse length is large enough to enable multiple returning trajectories. While we present the results obtained from the direct Fourier transform $a(\omega)$ of the dipole acceleration, we have confirmed the application of a Welch or Bartlett window [15] in the transformation hardly affects the results except for a constant factor. The HHG yield (defined as radiated energy per unit time [16]) integrated from 20 to 50 eV,

$$\Delta I = \frac{1}{3c^3}\int_{20\ \mathrm{eV}}^{50\ \mathrm{eV}} |a(\omega)|^2 d\omega, \qquad (2)$$

calculated on a coarse mesh in λ with a spacing of 50 nm (Fig. 1) falls off with a power law, $\Delta I \propto \lambda^{-x}$ ($x \approx 4.8$–5.5) for H and Ar, in qualitative agreement with Ref. [9]. The two alternative integration algorithms employed in this work agree well with each other. Small discrepancies near 2 μm are due to the difference in grid spacing and can be controlled by changes in the spacing near the origin. A power law ($x \approx 5$) results from the combination of two effects: the spreading of the returning wave packet would give $x = 3$ [6] for the overall yield. The increase of the cutoff $E_c \propto \lambda^2$ results for a fixed energy interval [see Eq. (2)] in an additional factor λ^{-2}. In fact, when increasing the upper integration limit in Eq. (2) to infinity, the exponent of the power law decreases and reaches $x \approx 3.5$ to 3.6 for Ar and H, in closer agreement with Ref. [6].

A closer look at Fig. 1 reveals the remarkable feature that the harmonic yield does not vary smoothly with λ as may have been anticipated in the previous work [9], but strongly fluctuates. Slight change in fundamental wavelength may lead to variations of the yield by a factor of 2–6. Such rapid fluctuations imply that a reliable λ dependence can only be established by employing a much finer λ grid. Moreover, the notion of a simple power-law scaling itself is called into question and can apply, if at all, only after averaging over fluctuations. The fluctuations are not specific to hydrogen but appear for argon [Fig. 1(b)] as well.

Figure 2 presents a two-dimensional zoom into the fine-scale variations calculated on a mesh with $\Delta\lambda = 1$ nm, as a function of λ and the photon energy E. Fluctuations appear which form vertical "ridges" spanning several harmonic orders. Consequently, after integrating over vertical strips we arrive at a fluctuating function $\Delta I(\lambda)$ (upper panel). Such variations in quantities averaged over a large energy interval are expected when few (quantum) orbits with a well-defined time structure significantly influence the spectrum ("periodic orbit spectra") [17]. A superposition of oscillations of different frequencies emerges (Fig. 3), the dominant of which has a fluctuation scale $\delta\lambda$ of $\approx$20 nm near a driver wavelength of $\lambda = 1000$ nm, and $\delta\lambda \approx 6$ nm near $\lambda = 2000$ nm. Similar oscillation patterns can be observed for argon in Fig. 3(c). Appar-

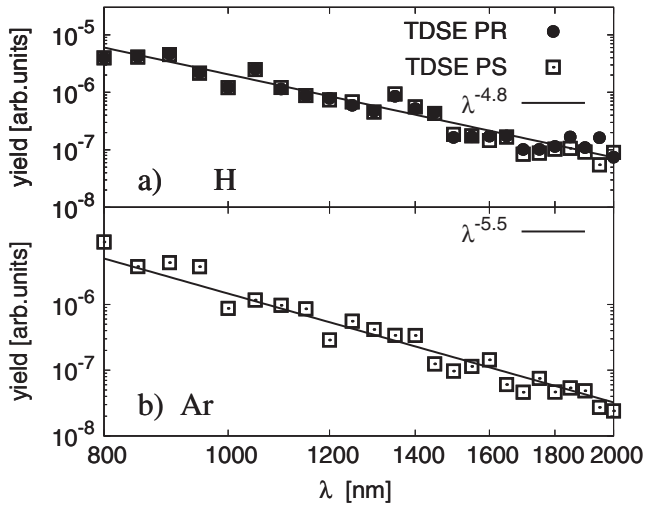

FIG. 1. Integrated harmonic yield ΔI between 20 and 50 eV as a function of λ calculated on a coarse mesh with $\Delta\lambda = 50$ nm. (●) Peaceman-Rachford (PR) method, (□) pseudospectral (PS) method. (Solid line) fit $\Delta I \propto \lambda^{-x}$: (a) hydrogen, (b) argon.

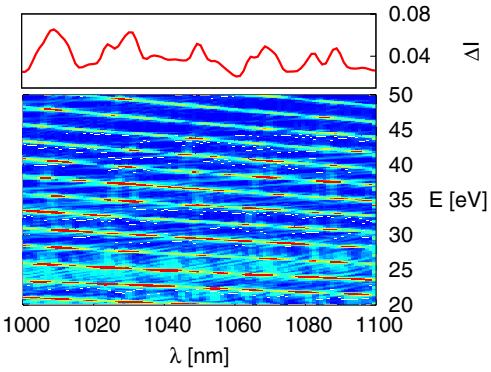

FIG. 2 (color online). Fluctuations of the harmonic yield ΔI as a function of the fundamental wavelength λ and the photon energy E for hydrogen. An oscillatory behavior of the yield as a function of λ emerges after integrating over vertical strips [upper panel and Fig. 3(a)].

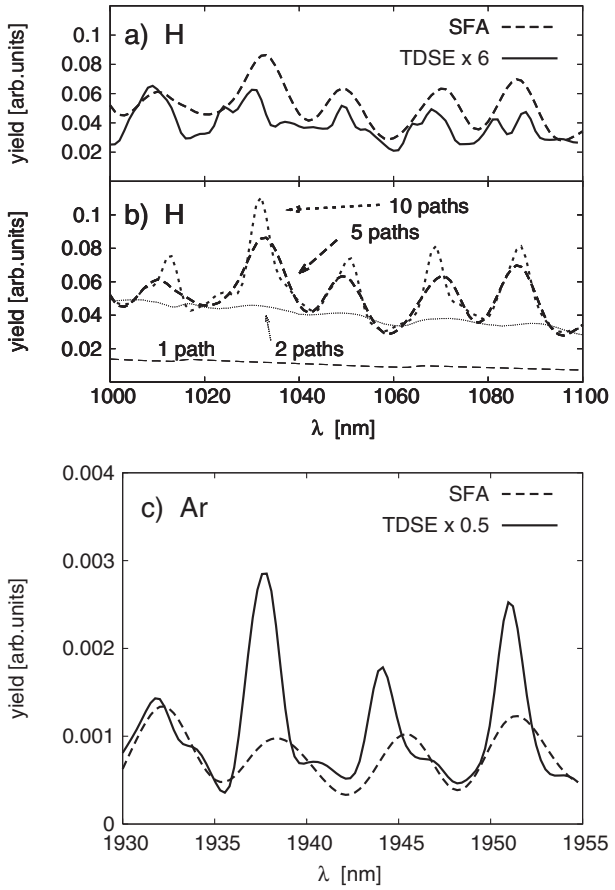

FIG. 3. Variations in the integrated harmonic yield (20–50 eV) in a narrow range of λ. (a) Comparison between the TDSE solution with the SFA including 5 quantum paths for hydrogen. (b) Build up of the interference pattern with increasing number of quantum trajectories within the SFA. Thin dashed line: 1 (short) trajectory, thin dotted line: 2 (short and long) trajectories, bold dashed line (dotted line): inclusion of the shortest 5 (10) trajectories. (c) as (a) but for argon.

ently, they are largely independent of the atomic species. Such oscillations are obviously the result of interference effects.

Many features of HHG can be intuitively and even quantitatively explained in terms of quantum trajectories [6,18] which represent the semiclassical three step model [19]. The main contribution to the HHG spectrum comes from those electronic quantum paths that correspond to classical returning trajectories ionized at a certain time t_i and recombining with the parent ion at a later time t_f. In order to identify the origin of the interference structures we apply a semiclassical model based on the SFA [6,20]. In this model, the time-dependent dipole moment $d(t)$ can be expressed as [20]

$$d(t_f) = \sum_{P(t_i)} b_{\text{ion}}(t_i) e^{-iS_P(t_i,t_f)} c_{\text{rec}}(t_f) + \text{c.c.}, \qquad (3)$$

i.e., a sum over paths P that start at the moment of tunnel ionization t_i with amplitude $b_{\text{ion}}(t_i)$, evolve in the laser field, $e^{-iS_P(t_i,t_f)}$, and recombine upon rescattering at the core at time t_f with the amplitude $c_{\text{rec}}(t_f)$. The sum over all possible electron trajectories recolliding at time t_f may be large, but in practice is limited by wave packet spreading. We consider up to 16 possible ionization times t_i for each individual t_f.

Interference oscillations are controlled by the evolution phase, the semiclassical action of the path P, which reads

$$S_P(t_i, t_f) = \int_{t_i}^{t_f} \frac{(p + A(t'))^2}{2} dt' + g|E_i|(t_f - t_i), \qquad (4)$$

$|E_i|$ is the ionization potential (binding energy) of the atom and $A(t)$ the laser vector potential defined by $A(t) = -\int_t^T F(t')dt'$. p is the classical momentum of the returning trajectory, $g = 1.3$ is a correction factor that accounts for the dependence on the tunneling time, modifying the energy of the recolliding photons [6,21]. When including up to five returning paths, the semiclassical calculation can reproduce the modulation depth, modulation frequency, and the approximate phase of the λ oscillations reasonably well, thus unambiguously establishing the quantum path interference as the origin of the fluctuations [Fig. 3(b)]. Full convergence is only reached when up to 10 trajectories are included. Setting $g = 1.0$ yields only a phase shift of the predicted oscillations while retaining the modulation frequency and depth.

Very recently, first experimental evidence for the interference between the short and long paths was presented [22] in the *intensity dependence* of the HHG yield. Remarkably, for the present λ dependence the frequently discussed short and long trajectories [dotted curve in Fig. 3(b)] are insufficient to account for the interference oscillations. Moreover, the presence of the oscillations is independent of the particular choice of the envelope function $f(t)$. Note that the Fourier broadening of the few-cycle driving field exceeds, on a wavelength scale, the period $\delta\lambda$ of the modulation. This somewhat surprising finding is a direct consequence of the quantum path interference. As long as the few-cycle pulse permits the generation of a set of a few quantum paths in subsequent half-cycles, the overall temporal characteristics of the driver pulse are of minor importance, though the latter will influence the detailed shape of the interference pattern. Preliminary calculations for pulse propagation in one dimension, accounting for the geometric Guoy phase, show that interference oscillations persist in loose focus geometry.

The principal modulation length of the harmonic yield $\delta\lambda$ is a function of the wavelength λ itself. It approaches ≈ 6 nm near a wavelength of 2 μm (Fig. 4). For a simple estimate for the scaling of $\delta\lambda$ with λ we note that the semiclassical action in Eq. (4) has its largest contribution from the $A(t)^2$ term in the strong field case. Hence, the phase difference between the shortest and longer trajectories due to the semiclassical action can be approximated by

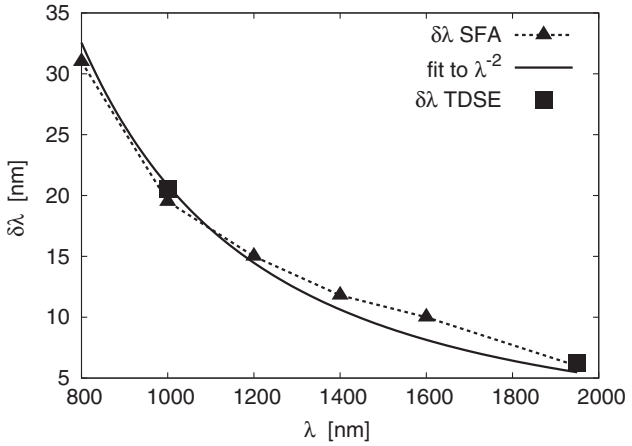

FIG. 4. Variation of the modulation period $\delta\lambda$ with the fundamental wavelength λ for hydrogen. (■) TDSE, (▲) SFA. (Solid line) λ^{-2} scaling [see Eq. (6)].

$\bar{S}_P \approx U_p \tau_f$, where $\tau_f = t_f - t_i$ is the flight time of the electron trajectory [18]. $\bar{S}_P$ scales approximately as λ^3. The period of the modulation corresponds to a phase change of $\bar{S}_P$ by 2π. Accordingly,

$$2\pi = \delta\bar{S}_P = \frac{dS}{d\lambda}\delta\lambda, \tag{5}$$

or

$$\delta\lambda \propto \lambda^{-2}. \tag{6}$$

This estimate can be improved when using the full expression for S_P; nevertheless, even Eq. (6) predicts the λ dependence of the modulation length remarkably well (see Fig. 4). Small-scale changes of HHG yield at variation of intensity have also been observed near channel closings [23], leading also to strong contributions of a large number of quantum orbits.

In conclusion, we have found that the fundamental wavelength dependence of HHG in the single-atom response features surprisingly strong oscillations on fine wavelength scales with modulation periods as small as 6 nm in the midinfrared regime near $\lambda = 2\ \mu$m. These oscillations have been established for both hydrogen and rare gas targets (as an example argon is shown in this work) using two complementary integration algorithms for the TDSE. Thus, even a slight change in fundamental wavelength leads to variations in the HHG yield by a factor of up to ≈ 6. According to our semiclassical analysis based on the SFA, this unexpectedly rapid variation on a fine scale is the consequence of the interference of different rescattering trajectories. We have to take account of up to five returns to reproduce the results of the quantum simulations. This confirms the significance of higher-order returns of the electron wave packet [9]. On a large λ scale, apart from the rapid oscillation, our TDSE results show that the HHG yield at constant intensity decreases as λ^{-x} with $x \approx 5$ for H and Ar. This dependence is different from the generally accepted λ^{-3} scaling, but is close to that reported in Ref. [9].

The work was supported by the Austrian Fonds zur Förderung der wissenschaftlichen Forschung, under Grant No. FWF-SFB016 "ADLIS." K. S. also acknowledges support by the IMPRS-APS program of the MPQ (Germany). K. L. I. gratefully acknowledges financial support by the Precursory Research for Embryonic Science and Technology (PRESTO) program of the Japan Science and Technology Agency (JST) and by the Ministry of Education, Culture, Sports, Science, and Technology of Japan, Grant No. 19686006.

*klaus@concord.itp.tuwien.ac.at

[1] J. Seres *et al.*, Nature (London) **433**, 596 (2005).
[2] M. Hentschel *et al.*, Nature (London) **414**, 509 (2001).
[3] G. Tsakiris *et al.*, Nature (London) **426**, 267 (2003).
[4] T. Sekikawa, A. Kosuge, T. Kanai, and S. Watanabe, Nature (London) **432**, 605 (2004).
[5] Y. Nabekawa, H. Hasegawa, E. J. Takahashi, and K. Midorikawa, Phys. Rev. Lett. **94**, 043001 (2005).
[6] M. Lewenstein, Ph. Balcou, M. Yu. Ivanov, A. L'Huillier, and P. B. Corkum, Phys. Rev. A **49**, 2117 (1994).
[7] A. Gordon and F. Kärtner, Opt. Express **13**, 2941 (2005).
[8] B. Shan and Z. Chang, Phys. Rev. A **65**, 011804(R) (2001).
[9] J. Tate *et al.*, Phys. Rev. Lett. **98**, 013901 (2007).
[10] H. G. Muller and F. C. Kooiman, Phys. Rev. Lett. **81**, 1207 (1998).
[11] K. C. Kulander, K. J. Schafer, and J. L. Krause, in *Atoms in Intense Laser Fields*, edited by M. Gavrila (Academic, New York, 1992), pp. 247–300.
[12] J. L. Krause, K. J. Schafer, and K. C. Kulander, Phys. Rev. A **45**, 4998 (1992).
[13] X.-M. Tong and S. Chu, Chem. Phys. **217**, 119 (1997).
[14] K. Schiessl, E. Persson, A. Scrinzi, and J. Burgdörfer, Phys. Rev. A **74**, 053412 (2006).
[15] W. H. Press *et al.*, *Numerical Recipes* (Cambridge University Press, Cambridge, 1992).
[16] J. D. Jackson, *Classical Electrodynamics* (John Wiley & Sons, New York, 1998).
[17] M. L. Du and J. B. Delos, Phys. Rev. Lett. **58**, 1731 (1987).
[18] P. Salières *et al.*, Science **292**, 902 (2001).
[19] P. B. Corkum, Phys. Rev. Lett. **71**, 1994 (1993).
[20] M. Yu. Ivanov, T. Brabec, and N. Burnett, Phys. Rev. A **54**, 742 (1996).
[21] V. Yakovlev and A. Scrinzi, Phys. Rev. Lett. **91**, 153901 (2003).
[22] A. Zaïr *et al.*, in *Proceedings of the XXVth International Conference on Photonic, Electronic and Atomic Collisions, Freiburg, Germany, 2007*, Abstract No. Mo046 (to be published).
[23] D. B. Milošević and W. Becker, Phys. Rev. A **66**, 063417 (2002).